

Delivering science and technology  
to protect our nation  
and promote world stability



Operated by Los Alamos National Security, LLC for the U.S. Department of Energy's NNSA

# Measurements on a Subcritical Copper-Reflected $\alpha$ -phase Plutonium (SCR $\alpha$ P) Sphere

J. Hutchinson, R. Bahran, T. Cutler, W. Monange\*, J. Arthur,  
M. Smith-Nelson, E. Dumonteil\*

Los Alamos National Laboratory

*\*Institut de Radioprotection et de Sûreté Nucléaire (IRSN)*



ANS Winter 2017



# Overview

- Introduction
- Experiment Design
- Experiment Overview
- **Preliminary** Results
- Future work

# Introduction

# Design/Conduct/Analyze Subcritical Validation Experiments

## ○ Nuclear Data and Transport Codes

- Fill integral experiment database deficiencies

+

- Find differential nuclear data library deficiencies

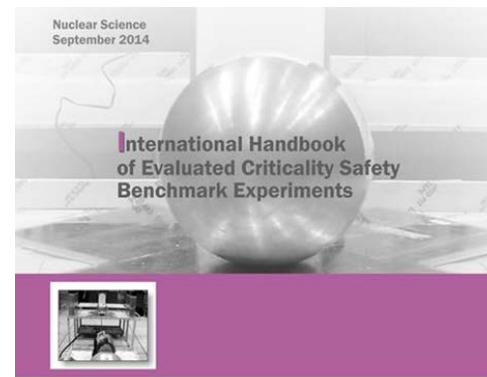
For different....

- Energy Ranges (Thermal, Intermediate, Fast)
- Multiplication Ranges (Low, Medium, High)
- Materials (Fissile, Moderator, Reflector)
- Neutron Reactions

## ○ Uncertainty Quantification

# Recent Advances in Subcritical Experiments

- We have come a long way since the first subcritical measurements at CP-1 in 1942.
- Many organizations (LANL, LLNL, SNL, IAEA, IRSN, CEA, universities, and others) have pursued subcritical experiments and/or simulations in recent years.
- The BeRP ball reflected by nickel benchmark evaluation was published in the 2014 edition of the ICSBEP handbook.
- This benchmark was the first:
  - Published benchmark evaluation of measurements performed at DAF.
  - Benchmark evaluation using new MCNP® capabilities for subcritical systems (the MCNP5 list-mode patch and MCNP6 list-mode capabilities).
  - Benchmark using the Feynman Variance-to-Mean method.
  - LANL-led subcritical experiment in the ICSBEP handbook.
- This benchmark was the culmination of several years of subcritical experiment research.
- BeRP-tungsten published in 2016 edition of ICSBEP handbook.



# Experiment Design

# Experiment Design

- **SCRaP Experiment Design**

- BeRP (Beryllium-Reflected Plutonium).
  - 4.5-kg WG  $\alpha$ -phase stainless-steel clad plutonium sphere.
  - Originally used in Be-reflected critical experiment (no Be was present for this experiment).
- High-purity nested copper shells
  - C101 Cu alloy (99.99 wt.% Cu).





# Experiment Design

- **SCRaP Experiment Design**
  - High-density interleaved polyethylene shells
- **Wide range of achievable subcritical multiplication values will help:**
  - Identify deficiencies and quantify uncertainties in nuclear data
  - Validate computational methods related to neutron multiplication inference.



Two purposes for the configurations with polyethylene:

- Allows for higher multiplication factor than with copper alone
- Allows for a different neutron spectra (and resulting sensitivity) for the same multiplication factor.

# Experiment Design

- **NoMAD (Neutron Multiplicity  $^3\text{He}$  Array Detector)** was used to measure three benchmark parameters:
  - Detector singles count rate ( $R_1$ ) i.e. the count rate in the detector system
  - Doubles count rate ( $R_2$ ) i.e. the rate in the detector system in which two neutrons from the same fission chain are detected
  - Leakage multiplication ( $M_L$ ) i.e. the number of neutrons escaping a system per starter neutron.



Records list-mode data (a time list of every recorded neutron event to a resolution of 128 nsec).

Photograph and MCNP® model of the NoMAD detector system.

15 He-3 tubes inside polyethylene.

# Experiment Design

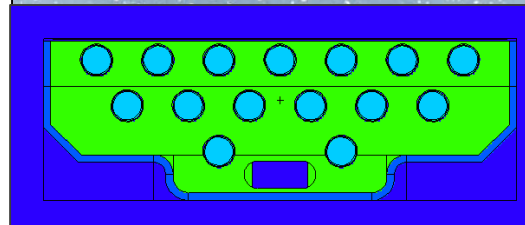


For the SCRaP experiment, two NoMAD systems were present and collected data in the same time list.



Records list-mode data (a time list of every recorded neutron event to a resolution of 128 nsec).

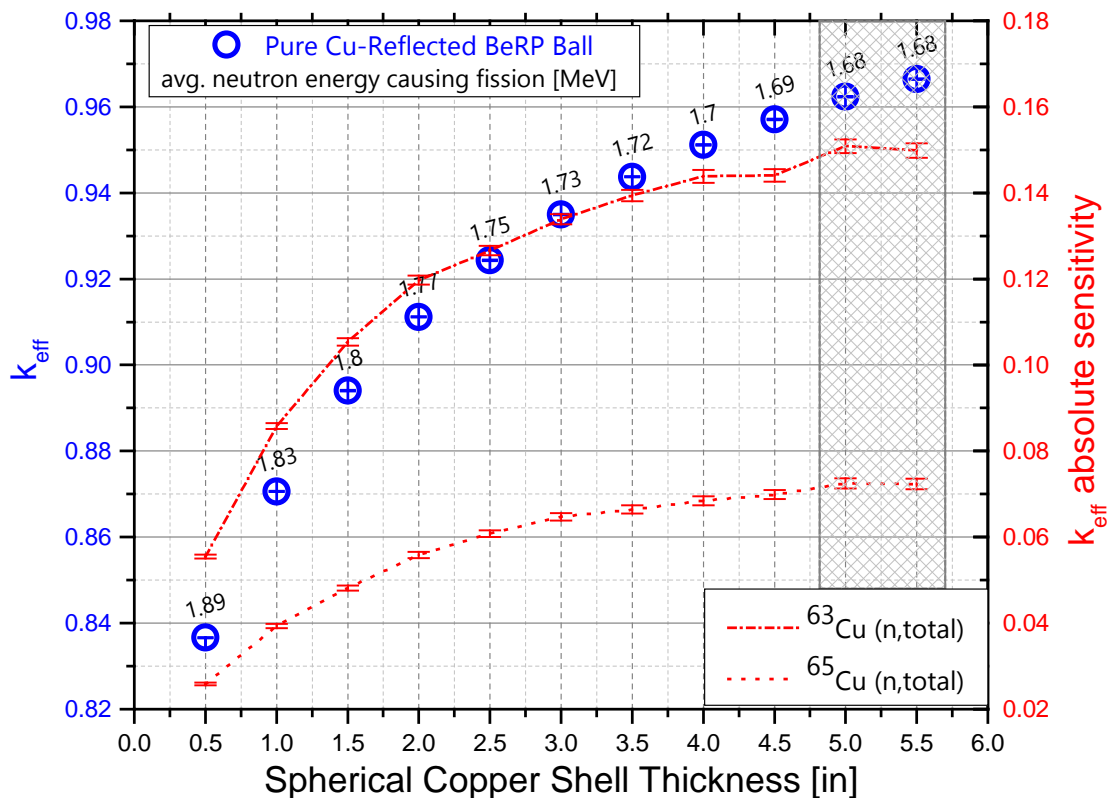
Photograph and MCNP® model of the NoMAD detector system.



15 He-3 tubes inside polyethylene.

# Experiment Design

- Final configurations were chosen based upon:
  - Criticality results
  - Sensitivity results: total
  - Sensitivity results: intermediate energy
  - Average neutron energy causing fission
  - Cost
  - Criticality safety
  - Practicality (weight of shells, etc.)
- Described in detail in an experimental design document.



# Experimental Design

- Experimental uncertainties for 4 experimental parameters were calculated.
- Used criticality eigenvalue calculations for these estimates as described in a previous work [J. HUTCHINSON, T. CUTLER “Use of Criticality Eigenvalue Simulations for Subcritical Benchmark Evaluations” Transactions of the ANS Winter Meeting, Las Vegas NV (2016)].

Many lessons-learned from the previous Ni and W benchmarks were used to minimize experimental uncertainties.

Estimate of experimental uncertainties for Configuration 15 (0.5 inch-thick HDPE surrounded by 3.5 inch-thick copper).

Parameter	Experimental Uncertainty	Uncertainty
M <sub>L</sub>	Pu radius ± 2 mils	0.18
	Pu isotopics ± 0.5%	0.19
	Cu thickness ± 0.3 cm	0.03
	Cu mass ± 0.5%	0.00006
R <sub>1</sub>	Pu radius ± 2 mils	1024
	Pu isotopics ± 0.5%	1045
	Cu thickness ± 0.3 cm	141
	Cu mass ± 0.5%	0.34
R <sub>2</sub>	Pu radius ± 2 mils	37450
	Pu isotopics ± 0.5%	41336
	Cu thickness ± 0.3 cm	5252
	Cu mass ± 0.5%	13.1

Cu mass was expected to be a minor uncertainty, which the table confirms.

# Experiment Overview

# Experiment configurations

- **17 total configurations:**
  - 1 Bare
  - 8 Cu-only configurations
  - 7 Cu+HDPE configurations
  - 1 HPDE-only configuration
- **In order to determine the detector efficiency, Cf-252 source replacement measurements were performed.**
  - The source strength of the <sup>252</sup>Cf source at the time of the measurements was 7.59e5 fissions/sec +/- 1.0%.



Configu ration #	Layer number (each layer is 0.5 inches thick)							
	1	2	3	4	5	6	7	8
0								
1								
2								
3								
4								
5								
6								
7								
8								
9								
10								
11								
12								
13								
14								
15								
16								

Orange is for Cu  
Grey is for HDPE



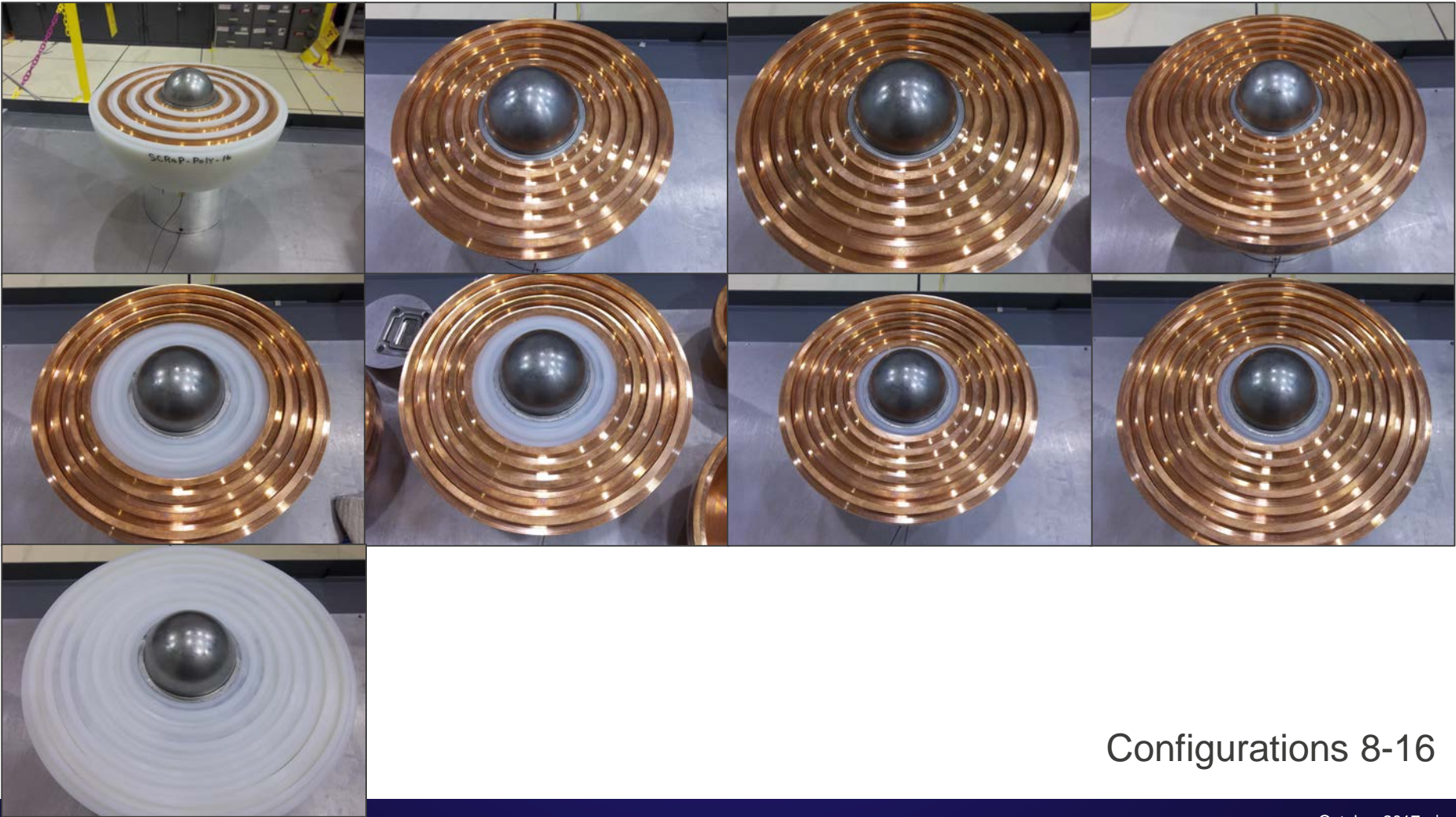
# Experiment configurations



Configurations 0-7

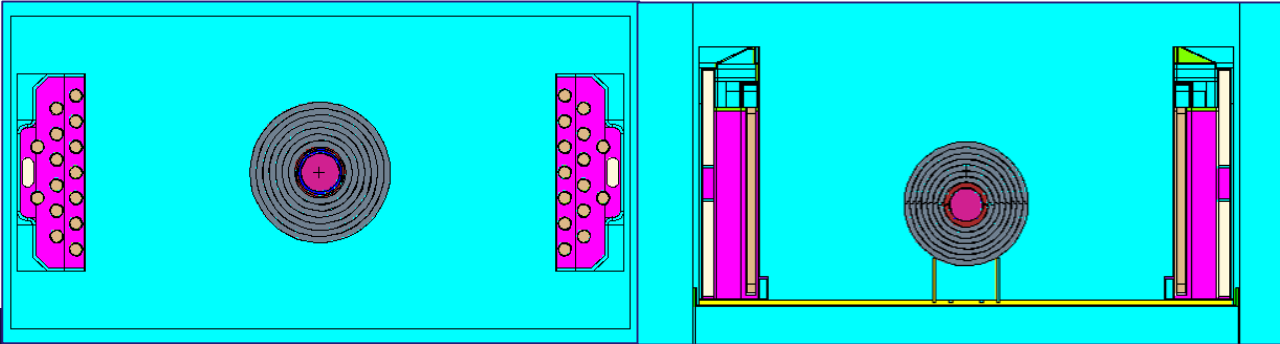


# Experiment configurations



Configurations 8-16

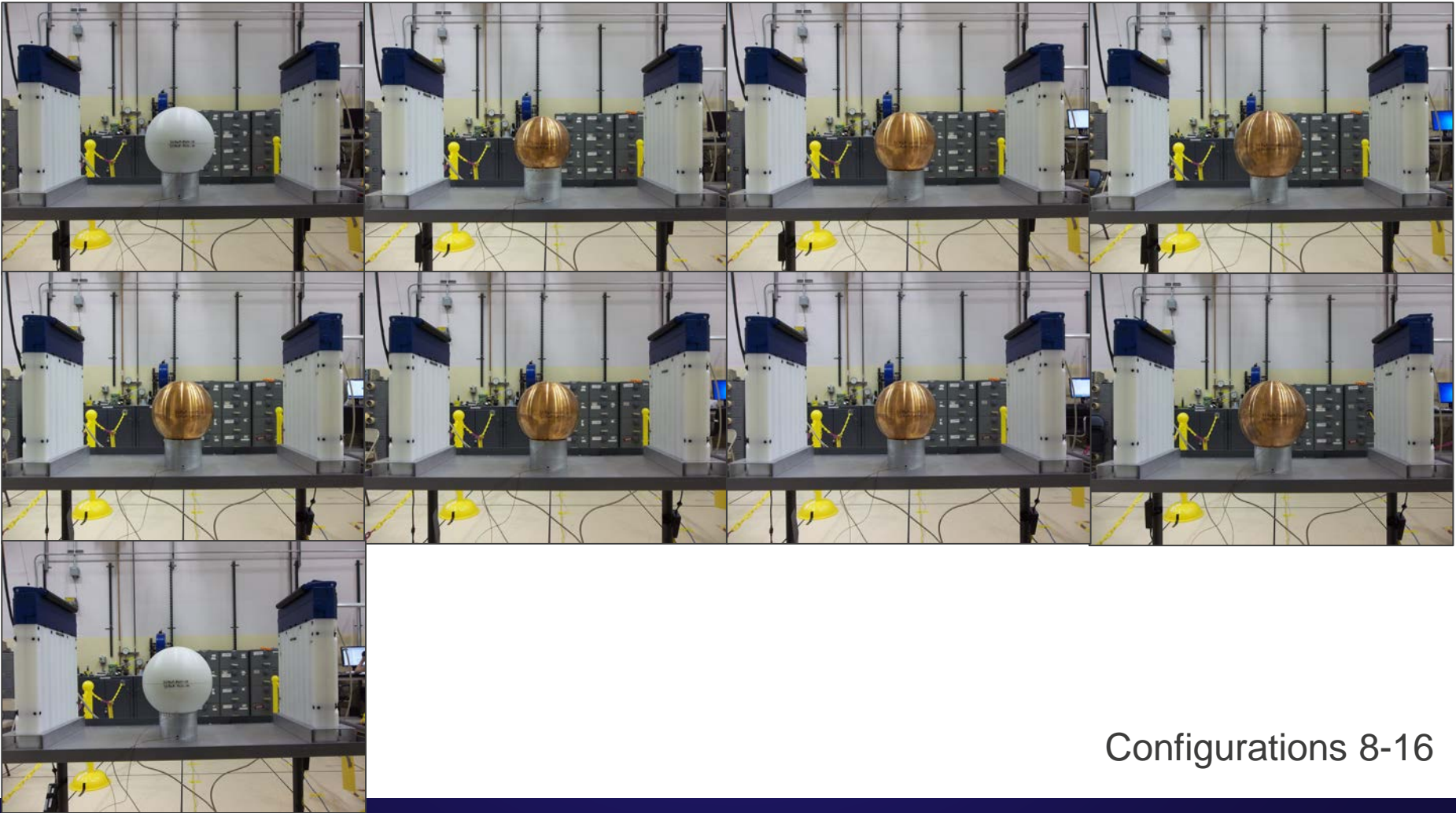
# Experiment configurations



Configurations 0-7



# Experiment configurations



Configurations 8-16

# Preliminary Results

# Analysis method

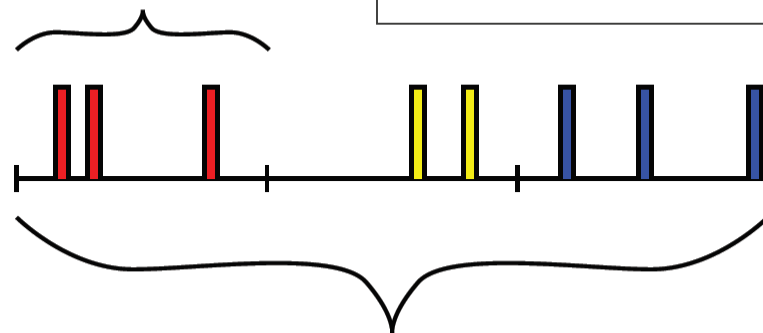
- **Neutron noise analysis**

- Rossi-alpha
- Time interval analysis
- Feynman variance to mean
  - Hansen Dowdy
  - [Hage-Cifarelli](#)
- Others...

- **Analysis method used here is documented in detail in the BeRP/Ni and BeRP/W ICSBEP evaluations.**

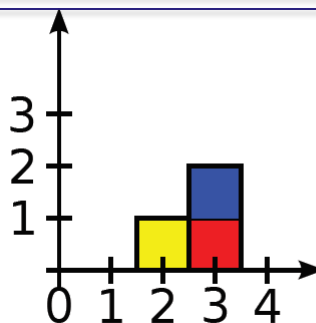
gate width,  $\tau$

Data are separated into gates (of time-width  $\tau$ )



count time,  $t$

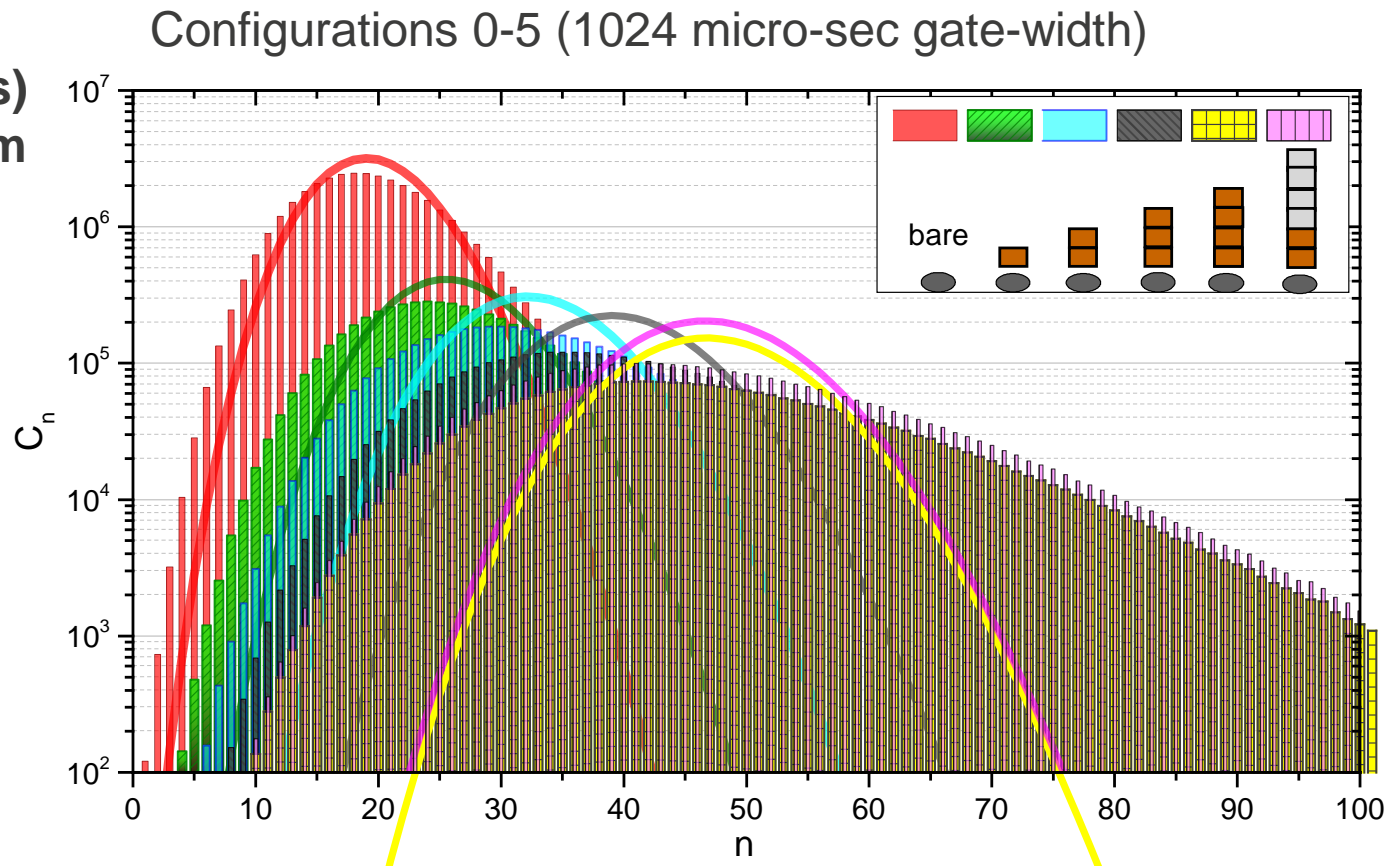
y-axis is the number of gates that contained exactly  $n$  events ( $C_n$ )



x-axis is the number of neutrons recorded in the gate ( $n$ )

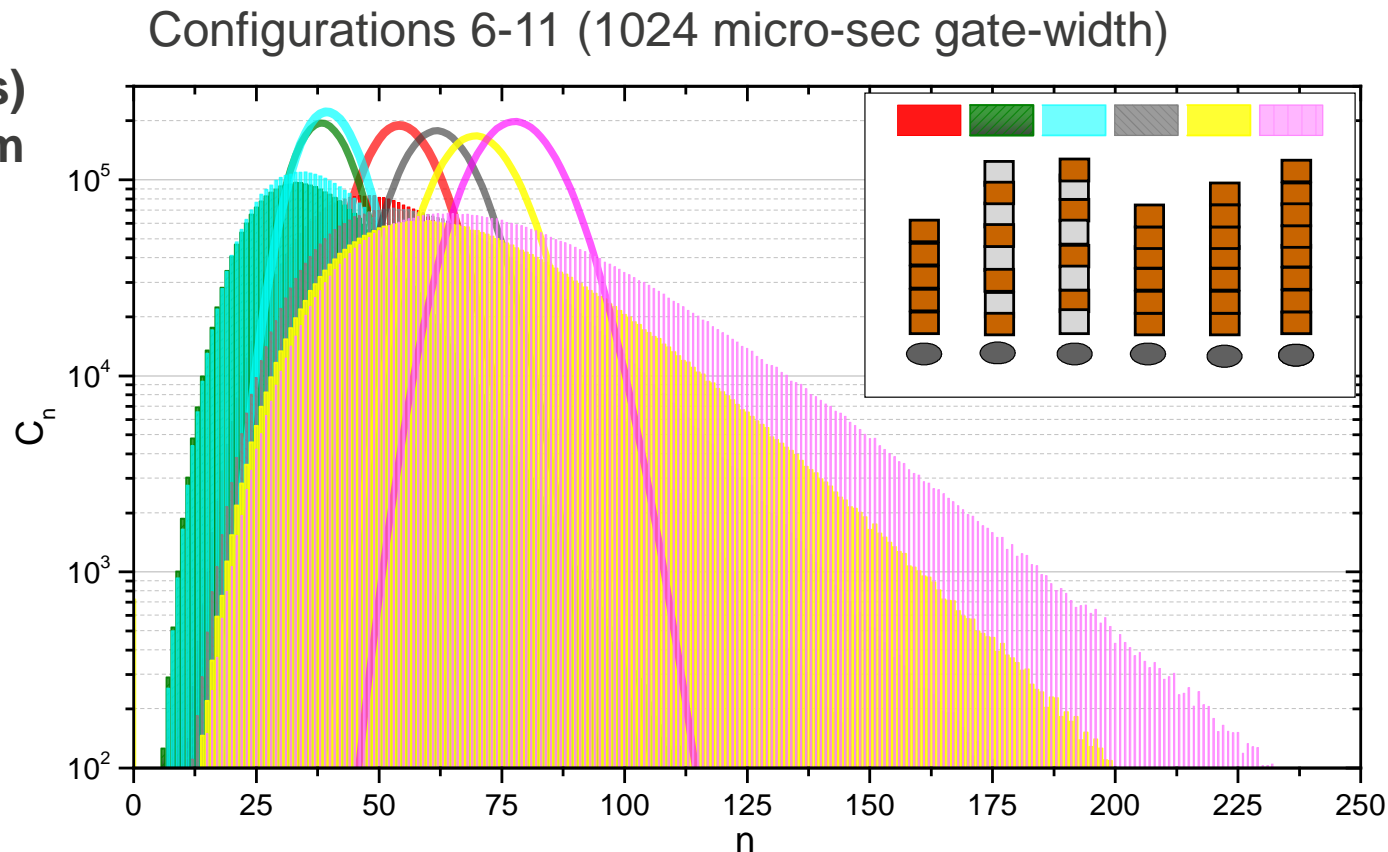
# Feynman histogram results

- Deviation from Poisson (solid lines) increases as system multiplication increases.
- Mean of histogram is proportional to the detector count rate.
- Width of histogram is proportional to the doubles count rate.



# Feynman histogram results

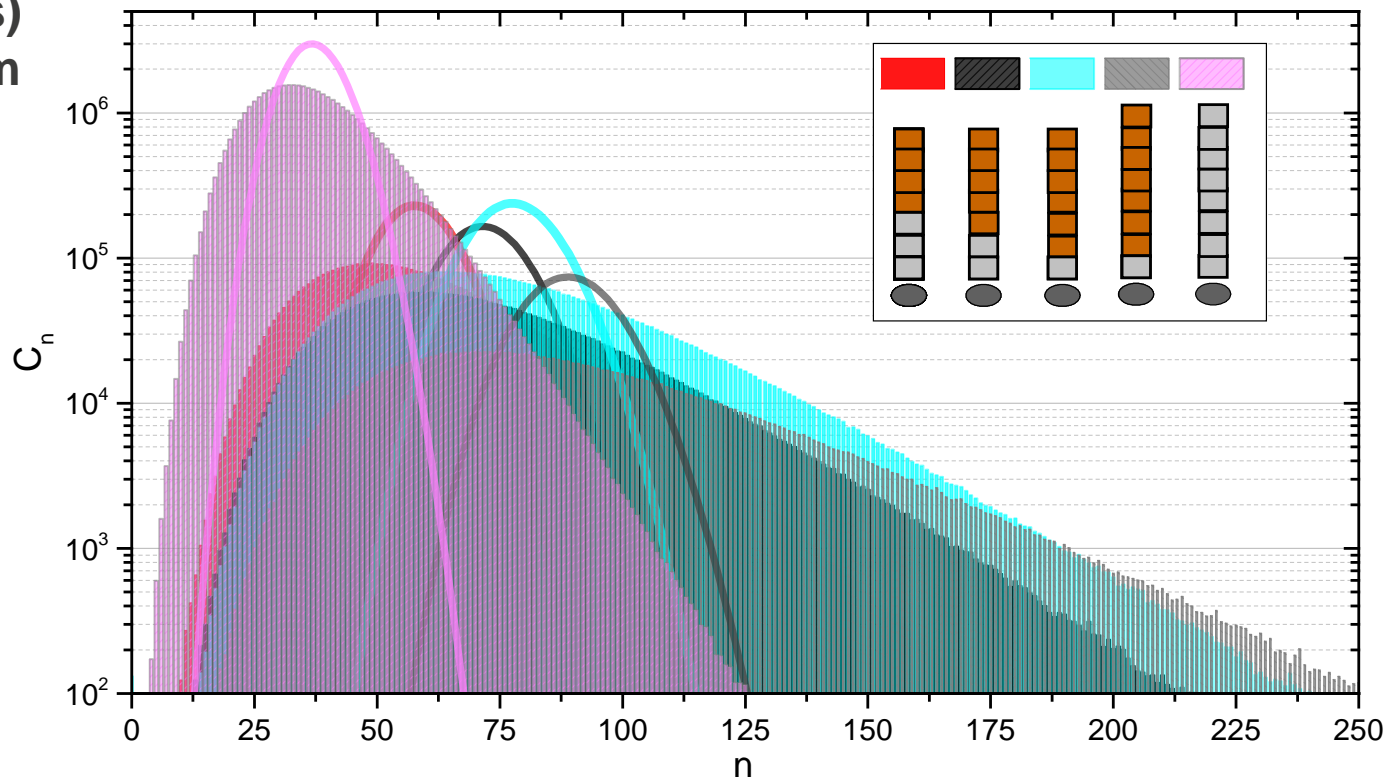
- Deviation from Poisson (solid lines) increases as system multiplication increases.
- Mean of histogram is proportional to the detector count rate.
- Width of histogram is proportional to the doubles count rate.



# Feynman histogram results

- Deviation from Poisson (solid lines) increases as system multiplication increases.
- Mean of histogram is proportional to the detector count rate.
- Width of histogram is proportional to the doubles count rate.

Configurations 12-16 (1024 micro-sec gate-width)





# Singles count rate ( $R_1$ )

Reduced factorial moment:

$$m_r(\tau) = \frac{\sum_{n=0}^{\infty} n(n-1)\cdots(n-r+1)p_n(\tau)}{r!}$$

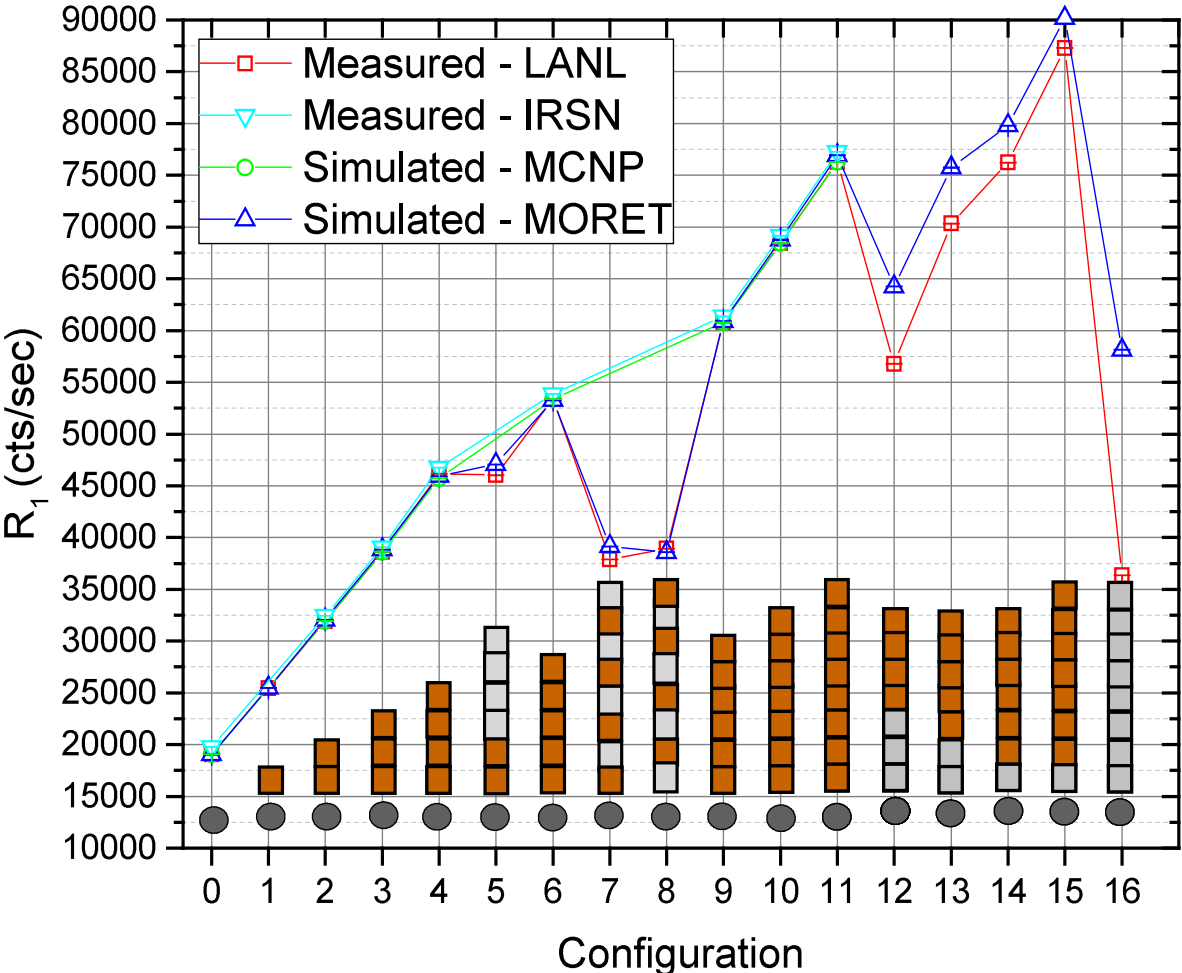
normalized fraction of gates that recorded n events:

$$p_n(\tau) = \frac{C_n(\tau)}{\sum_{n=0}^{\infty} C_n(\tau)}$$

Singles count rate:

$$R_1(\tau) = \frac{m_1(\tau)}{\tau}$$

Gate-width ( $\tau$ )



# Singles count rate ( $R_1$ )

Detector efficiency (from Cf-252 measurements):

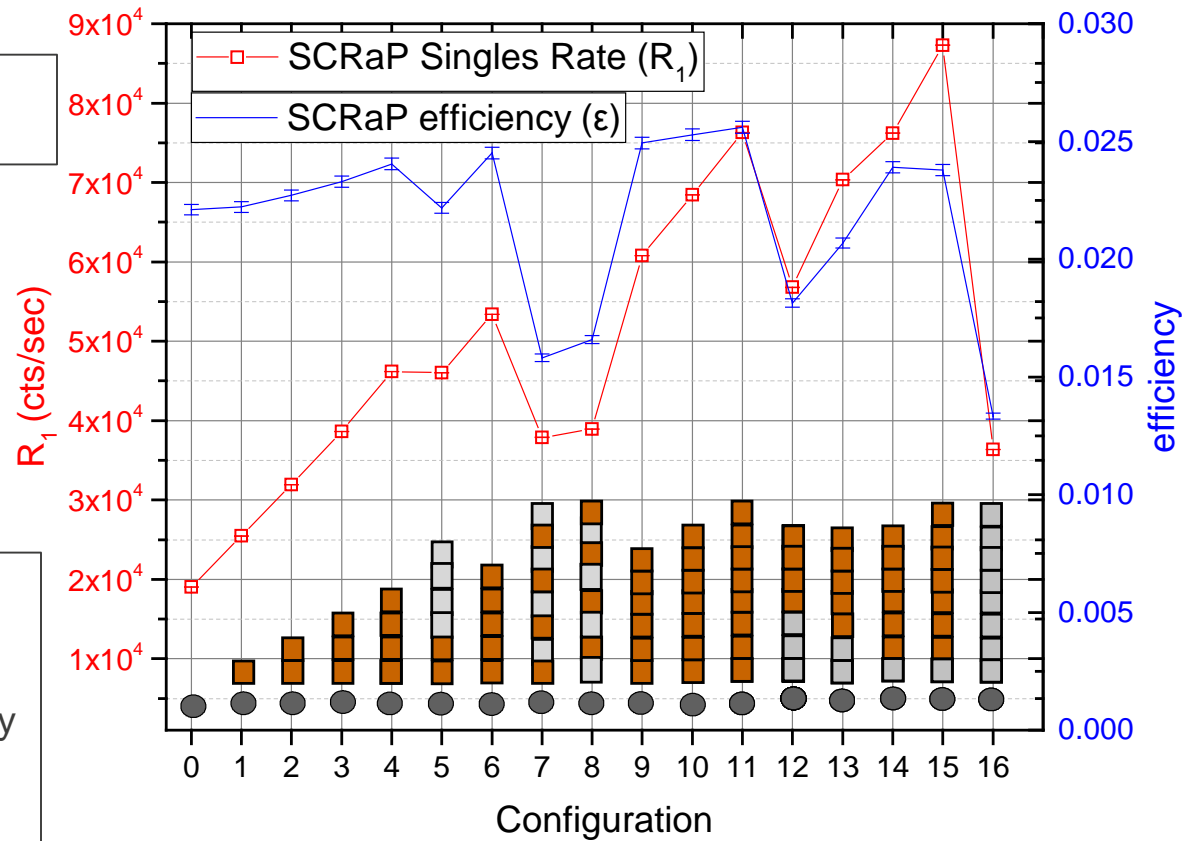
$$\varepsilon = \frac{R_1(\tau)}{F_S \bar{\nu}_{S(1)}}$$

This is the count rate from the Cf-252 measurements.

$F_S$  is the reported spontaneous fission emission rate of the  $^{252}\text{Cf}$  source.

$\bar{\nu}_{S(1)}$  is the average number of neutrons emitted per  $^{252}\text{Cf}$  fission.

Plotted together to show that the reason that the count rate goes down significantly for the configurations with HDPE is due to the decrease in efficiency (which is caused by neutron absorption primarily in the hydrogen).

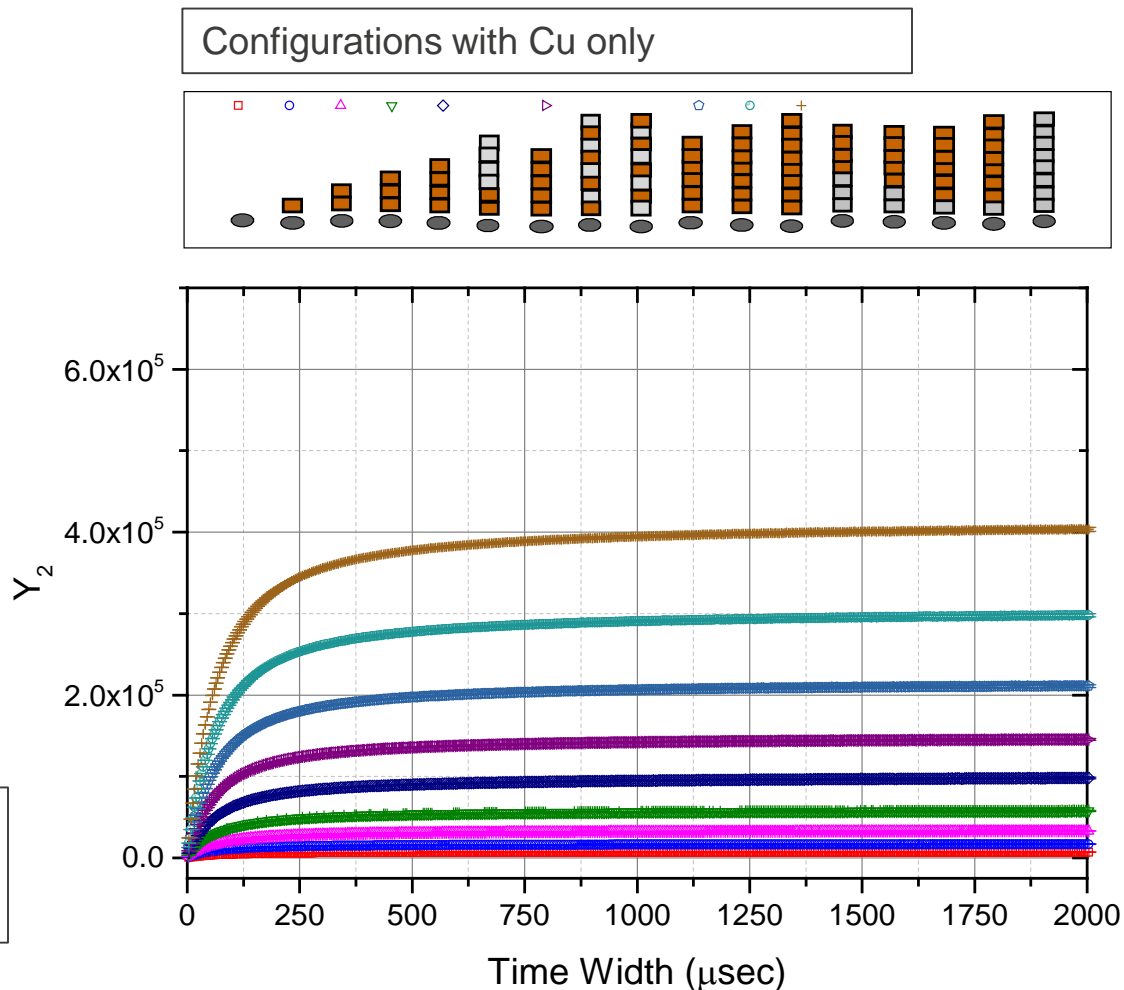


# Excess variance

The excess variance (deviation of a Feynman histogram from a Poisson distribution) is proportional to  $Y_2$ , given by:

$$Y_2(\tau) = \frac{m_2(\tau) - \frac{1}{2}[m_1(\tau)]^2}{\tau}$$

The amount of excess variance increases with Cu thickness (due to an increase in the system multiplication).



# Excess variance

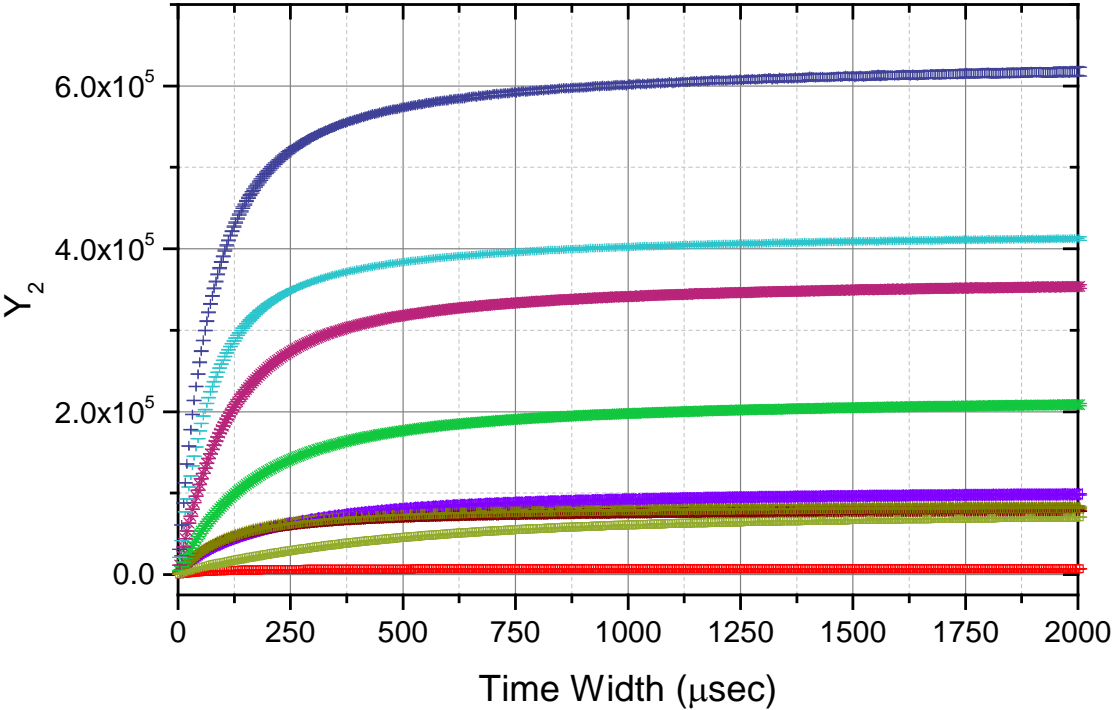
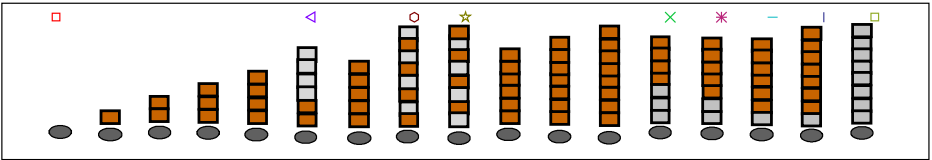
The excess variance (deviation of a Feynman histogram from a Poisson distribution) is proportional to  $Y_2$ , given by:

$$Y_2(\tau) = \frac{m_2(\tau) - \frac{1}{2}[m_1(\tau)]^2}{\tau}$$

The amount of excess variance increases with the system multiplication.

HDPE can increase or decrease  $Y_2$  (due to a competition between multiplication and detector efficiency (due to absorption in H)).

Configurations with Cu+HDPE

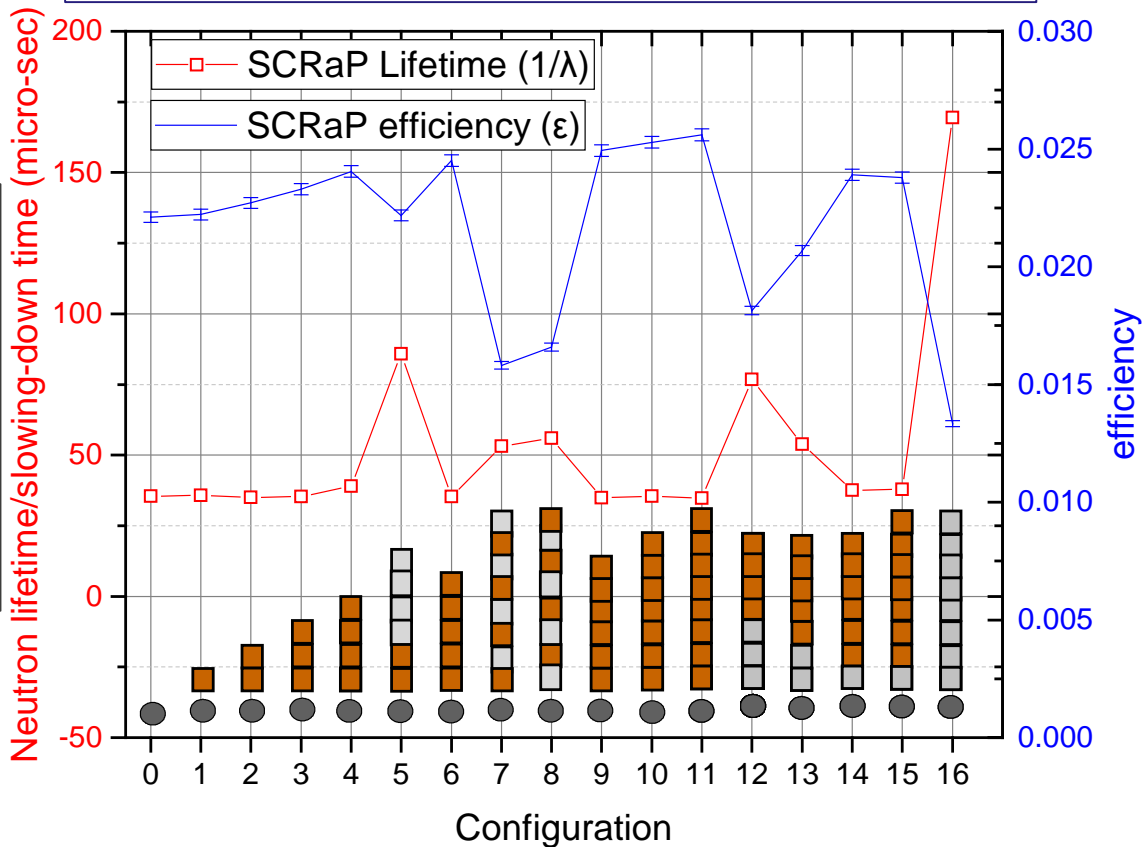


# Neutron lifetime/slowing-down time

Neutron lifetime/slowing-down time ( $1/\lambda$  or  $1/\alpha$ ) can be found by fitting either  $Y_2$  or Rossi- $\alpha$  data.

The focus of multiple talks during the morning crit/subcrit experiments session.

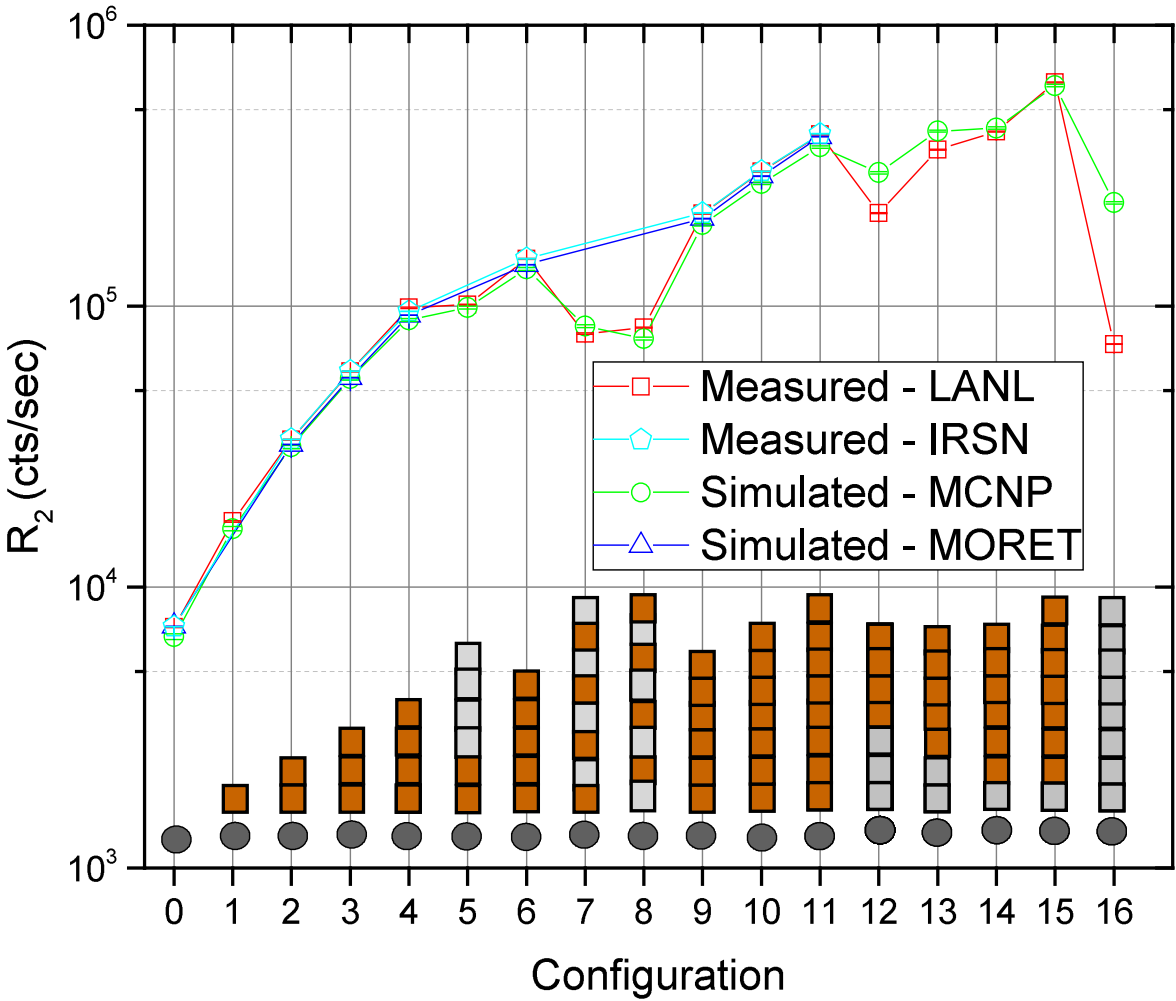
The NoMAD detector system has a slowing-down time of around 35 micro-seconds. For the configurations with Cu only, the result is approximately 35 micro-seconds as expected, but it is significantly larger for the configurations that include HDPE hemishells.



# Doubles count rate (R<sub>2</sub>)

Doubles count rate:

$$R_2(\tau) = \frac{Y_2(\tau)}{\omega_2(\lambda, \tau)}$$



# Leakage multiplication ( $M_L$ )

$$M_L = \frac{-C_2 + C_4}{2C_1}$$

with

$$C_1 = \frac{\bar{\nu}_{S(1)}\bar{\nu}_{I(2)}}{\bar{\nu}_{I(1)} - 1}$$

$$C_2 = \bar{\nu}_{S(2)} - \frac{\bar{\nu}_{S(1)}\bar{\nu}_{I(2)}}{\bar{\nu}_{I(1)} - 1}$$

$$C_3 = -\frac{R_2(\tau)\bar{\nu}_{S(1)}}{R_1(\tau)\varepsilon}$$

$$C_4 = \sqrt{C_2^2 - 4C_1C_3}$$

$\bar{\nu}_{S(1)}$  1st factorial moment of  $^{240}\text{Pu}$   $P_v$

$\bar{\nu}_{S(2)}$  2nd factorial moment of  $^{240}\text{Pu}$   $P_v$

$\bar{\nu}_{I(1)}$  1st factorial moment of  $^{239}\text{Pu}$   $P_v$

$\bar{\nu}_{I(2)}$  2nd factorial moment of  $^{239}\text{Pu}$   $P_v$

Assumes that there are no emissions from ( $\alpha, n$ ) neutrons.

Leakage multiplication is related to the multiplication factor ( $k_{\text{eff}}$ ).

# Leakage multiplication ( $M_L$ )

$$M_L = \frac{-C_2 + C_4}{2C_1}$$

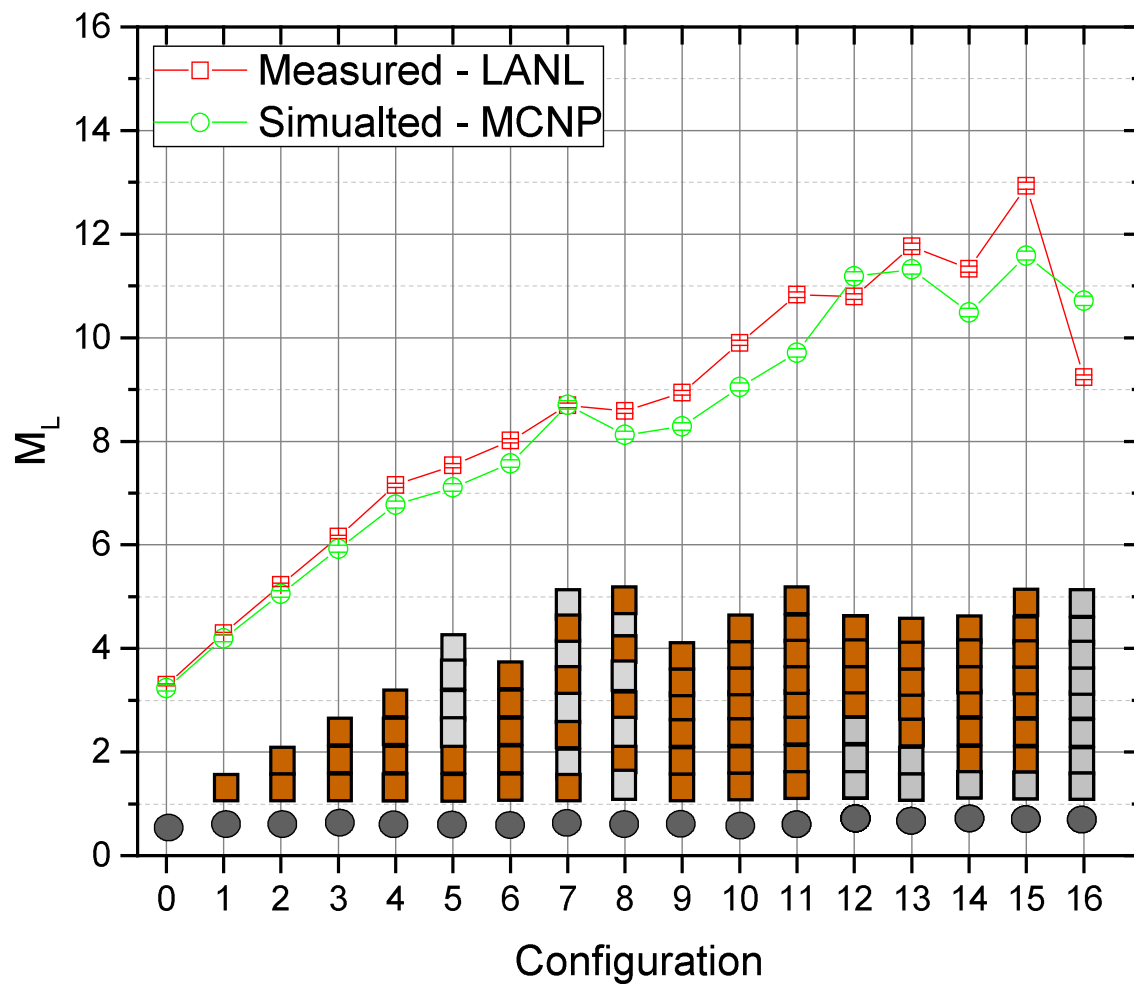
with

$$C_1 = \frac{\bar{v}_{S(1)} \bar{v}_{I(2)}}{\bar{v}_{I(1)} - 1}$$

$$C_2 = \bar{v}_{S(2)} - \frac{\bar{v}_{S(1)} \bar{v}_{I(2)}}{\bar{v}_{I(1)} - 1}$$

$$C_3 = -\frac{R_2(\tau) \bar{v}_{S(1)}}{R_1(\tau) \varepsilon}$$

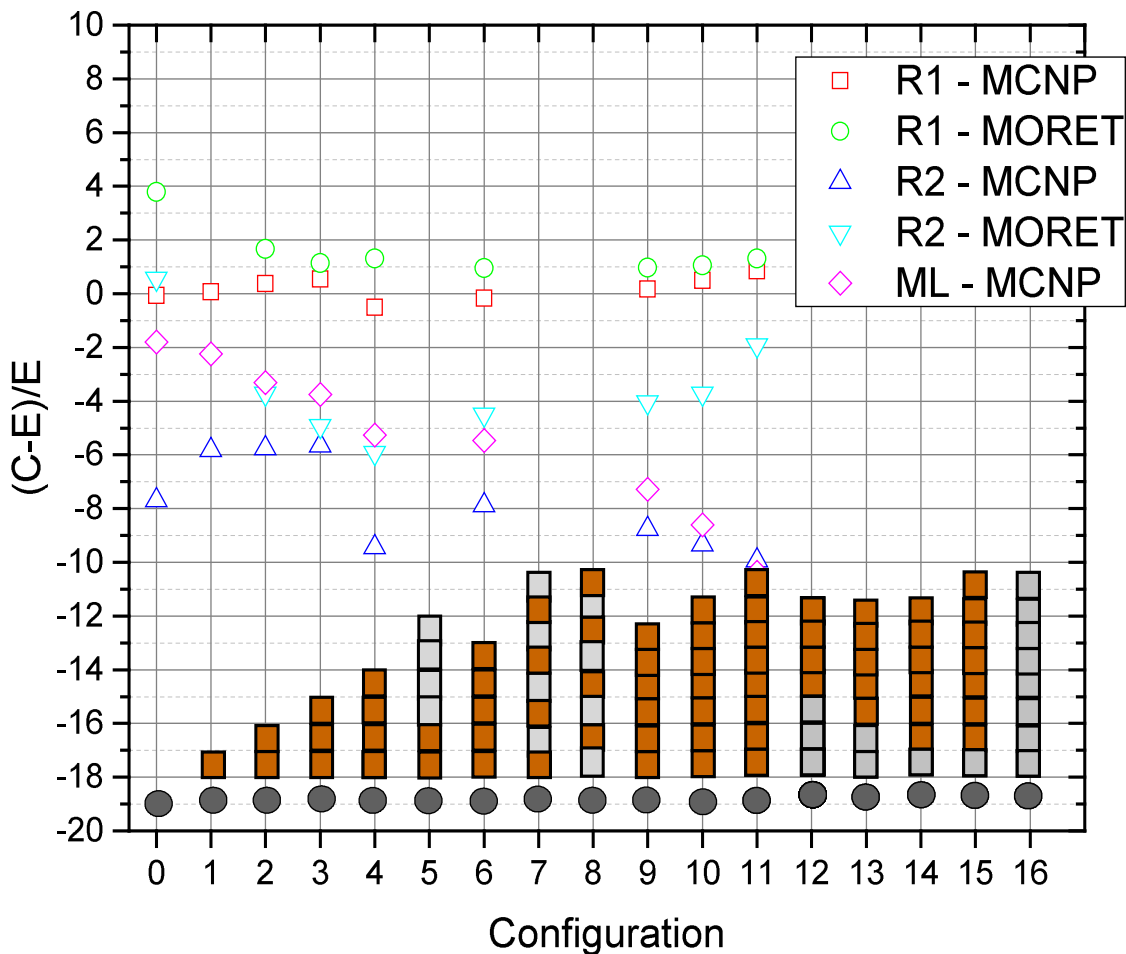
$$C_4 = \sqrt{C_2^2 - 4C_1 C_3}$$





# Measurement and simulation comparison

- MCNP simulations performed using MCNP 6.2.
- MORET simulations performed using MORET 5.D with neutron noise plugin.
- Both used ENDF/B-VII.1 cross-sections.



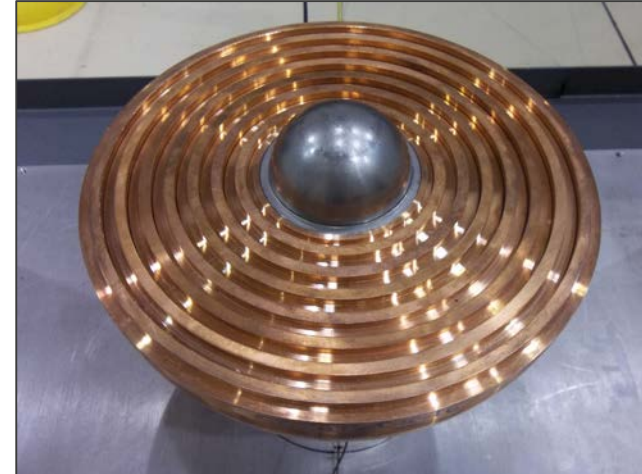
# Future work

# What's next?

- This experiment will be evaluated and documented in an upcoming version of the ICSBEP handbook.
- ALL parameters will be compared to simulated list-mode data.
- Simulations will be compared for a variety of codes (MCNP, Polimi, etc.) with correlated fission event generators (FREYA, CGMF) and various nuclear data libraries.
- Results will hopefully be used to improve cross-section libraries.
- Data set will also be used to validate subcritical analysis methods.



# Thank you for your attention.



**This work was supported by the DOE Nuclear Criticality Safety Program, funded and managed by the National Nuclear Security Administration for the Department of Energy.**